The Gauss-Poisson Process for Wireless Networks and the Benefits of Cooperation

Anjin Guo, *Student Member, IEEE*, Yi Zhong, *Student Member, IEEE*,
Wenyi Zhang, *Senior Member, IEEE*, and Martin Haenggi, *Fellow, IEEE*

***Abstract*—Gauss-Poisson processes (GPPs) are a class of clustered point processes, which include the Poisson point process as a special case and have a simpler structure than general Poisson cluster point processes. A key property of the GPP is that it is completely defined by its first- and second-order statistics. In this paper, we first show properties of the GPP and provide an approach to fit the GPP to a given point set. A fitting example is presented. We then propose the GPP as a model for wireless networks that exhibit clustering behavior and derive the signal-to-interference-ratio (SIR) distributions for different system models: (1) the basic model where the desired transmitter is independent of the GPP and all nodes in the GPP are interferers; (2) the non-cooperative model where the desired transmitter is one of the nodes in the GPP; (3) the cooperative model, where the nodes in a GPP cluster transmit cooperatively. The results indicate that a gain of 5-6 dB can be achieved with cooperation.**

I. Introduction

A. Motivation

Stochastic geometry tools have been widely used to analyze the performance of wireless networks [2]. A main application of stochastic geometry in wireless communication is to model the node locations using spatial point processes. With the point process models, metrics like success probability, average achievable rate, local delay and so on can be derived by quantitative analysis. When applying the point processes to model wireless networks, two key problems should be taken into consideration: first, whether a point process can accurately model the actual network which may employ medium access control; second, whether the point process model is tractable for analyzing the system performance.

Most of the works in the literature model wireless networks use the Poisson point process (PPP) [3]. This is because the PPP model has a number of convenient features, such as the independence between different points and the simple form of the probability generating functional (PGFL), which make the analysis tractable. But the PPP model may be inadequate for those scenarios where the node locations exhibit correlations.

A. Guo and M. Haenggi are with the Dept. of Electrical Engineering, University of Notre Dame, IN 46556 USA (e-mail: {aguo, mhaenggi}@nd.edu).

Y. Zhong and W. Zhang are with the Dept. of Electronic Engineering and Information Science, University of Science and Technology of China, Hefei 230027, China (e-mail: geners@mail.ustc.edu.cn; wenyizha@ustc.edu.cn).

Part of this work [1] was presented at the 2014 IEEE International Symposium on Information Theory (ISIT).

The research of A. Guo and M. Haenggi has been supported by the U.S. NSF (grants CCF-1216407 and CCF-1525904), and the research of Y. Zhong and W. Zhang has been supported by the National Basic Research Program of China (973 Program) through grant 2012CB316004 and the National Natural Science Foundation of China through grant 61379003.

In some circumstances, the transmitters form clusters, due to geographical factors (e.g., access points inside a building and groups of nodes moving in a coordinated fashion), or population factors (e.g., base stations in urban regions). Besides, the clustering phenomenon of transmitters can also be artificially induced by certain MAC protocols[1]. Thus, clustered point processes are suitable to model these transmitters' locations. A few prior studies have used models of clustered point processes, most notably, the Neyman-Scott process [6] [7]. In those works, the system performance indicators, such as success probability and mean achievable rate, are usually in complex form involving multiple integrals.

In this paper, we focus on the Gauss-Poisson process (GPP), which is a relatively simple clustered point process that has either one or two points in a cluster. As such, it retains a good level of tractability and constitutes a definitive improvement over the PPP in cases where "attraction" exists between node locations, and it achieves a good trade-off between modeling accuracy and tractability.

The motivation for introducing the GPP mainly comes from three aspects.

- The GPP belongs to the family of the Poisson cluster processes, with the number of points in each cluster restricted to one or two. It well describes the scenario where each cluster has one or a pair of nodes. In reality, scenarios where there are 1 or 2 transmitters close together are commonly seen including: 1) the scenario where one person uses a phone and a tablet to access the network concurrently, or two persons work together through their own devices; 2) some indoor deployments of access points where there are one or two access points of the cellular networks or Wi-Fi access points in one room; 3) full-duplex networks where each transceiver pair has a fixed/small inter-node distance [8]; 4) multi-antenna systems where each access point is equipped with two antennas; 5) military ad hoc networks, where each node represents a soldier and soldiers move in pairs for their missions. Not limited to model those scenarios, the (generalized) GPP is also suitable for many other types of clusters as will be pointed out in Section II.
- The generalized GPP, where the inter-point distance in each cluster is a random variable instead of a deterministic quantity, can be used in great generality to model the spatial distribution of transmitters based on first-order and

[1]Conversely, some MAC protocols may also lead to repulsion between transmitters [4], [5].

second-order statistics if the deployment of the transmitters appears clustered. It has been shown in [9] that this property makes the GPP the point process analog of the normal distribution, completely defined by its first- and second-order characteristics. This implies that a suitable GPP can be used to generate point distributions with any given intensity and two-point correlation function that satisfy certain constraints. In other words, given the first- and second-order statistics of an actual wireless network, we can use the GPP to model this network.
- The GPP constitutes a simple network model to analyze wireless networks that apply cooperative techniques (see Sections III-V).

B. Related Work

Both clustered point processes (e.g., the Neyman-Scott process) and repulsive point processes (e.g., the Ginibre point process and the Matérn hard-core processes) have been used to model wireless networks, including cellular networks. In [6], the authors derived the distributional properties of the interference and provide upper and lower bounds for its distribution, assuming the node locations form a Poisson cluster process on the plane. In [7], the Neyman-Scott process was used to model the distribution of femto-cells, and the distributions of the SINR and mean achievable rates of both nonsubscribers and subscribers were derived. In [10], the Ginibre point process was applied to cellular networks to model the locations of the base stations, and the interference and the coverage/success probability were analyzed. In [11], we used the Strauss process, the Poisson hard-core process and the perturbed triangular lattice to model actual base station locations in the UK.

The GPP has been well studied in the mathematical literature. In [12], the authors determined necessary and sufficient conditions on the first- and second-order measures for the resulting GPP point process to be well defined, and studied stationarity, ergodicity, and infinite divisibility of the GPP. In [9], the author proposed a simple method for the simulation of the GPP, given the intensity and the pair correlation function. Moreover, like the Poisson cluster processes, the GPP has also been used to model wireless networks. In [13], the GPP was proposed to fit a cognitive radio network based on the first- and second-order statistics using the method of minimum contrast, but no analysis was carried out using this model.

Recently, cooperative transmission techniques in cellular networks, known as coordinated multi-point transmission (CoMP), have been widely studied [14], [15]. For the downlink, CoMP can be divided into two categories: coordinated scheduling/beamforming [16], [17], which reduces inter-cell interference, and joint transmission (JT) [18]–[20]. In [18], the authors studied coherent JT with power-splitting in cellular networks where base stations cooperate in a pairwise manner. In [19], the authors proposed a tractable model for analyzing the base station cooperation of non-coherent JT, where the base stations follow a stationary PPP and at the receiver a received power boost is yielded by the non-coherent superposition of the useful signals. In [20], the authors considered the base station cooperation of both non-coherent JT and coherent JT in the downlink of heterogeneous cellular networks and derived the coverage/success probability.

C. Contributions

This work makes the following contributions:

- We propose an approach to using the GPP to model spatial distribution of wireless networks, for which the basic idea is to equalize both the first- and second-order statistics of the GPP and the point sets. A fitting case study is provided.
- We derive the SIR distributions for the following four models: (a) Basic model: the desired transmitter is independent of the GPP. (b) Non-cooperative model: the desired transmitter is a point of the GPP, and the other point in the same cluster (if any) acts as an interferer. (c) Cooperative model 1: the desired transmitter is a point of the GPP, the other point in the same cluster (if any) acts as a cooperator, and in the SIR expression at the receiver, the desired signals are combined by accumulating their powers. (d) Cooperative model 2: it is similar to the cooperative model 1, except that in the SIR expression at the receiver, the desired signal power is that of the sum of the amplitudes of the desired signals.
- We investigate the benefits of cooperative communications in a GPP network, which gives some fundamental insights into the benefits of cooperation techniques in large networks, where the interference from all transmitting nodes is properly accounted for.

II. The Gauss-Poisson Process

A. Definition

Definition 1 (Generalized Gauss-Poisson process [21])**.** *The generalized GPP is a Poisson cluster process with homogeneous independent clustering. The intensity of the parent process is denoted by $\lambda_{\rm p}$. Each cluster has one or two points, with probabilities $1-p$ and p, respectively. If a cluster has one point, it is located at the position of the parent. If a cluster has two points, one of them is at the position of the parent, and the other is randomly distributed around the parent with some PDF g.*

Note that in Def. 1, the inter-point distance u in the two-point cluster is random. If u is deterministic, which means that in two-point clusters, one point is at the position of the parent, and the other is uniformly distributed on the circle with radius u centered at the location of the parent, then the GPP is called a *standard* GPP as defined in [2, Example 3.8]. The standard GPP is motion-invariant (isotropic and stationary) [2, Ch. 2]. Fig. 1 shows a realization of a standard GPP with $\lambda_{\rm p} = 0.02$, $u = 1$ and $p = 0.5$.

Denote the parent point process of the generalized GPP by $\Phi_{\rm p} = \{x_1, x_2, ...\}$ with intensity $\lambda_{\rm p}$. Let $\{\Phi_x, x \in \Phi_{\rm p}\}$ be the clusters of the GPP, denoted by

$$\Phi_x = \begin{cases} \{x\} & \text{w.p. } 1-p \\ \{x, x+z_x\} & \text{w.p. } p, \end{cases} \tag{1}$$

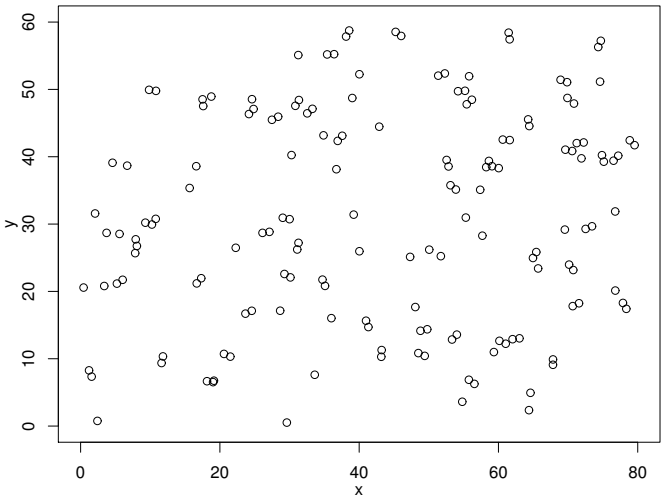

Fig. 1. A realization of the standard GPP on $[0,80]\times[0,60]$ with $\lambda_{\rm p}=0.02$, $u=1$ and $p=0.5$. There are in total 159 points. The expected number of points is $4800\times 0.02\times 1.5=144$.

The intensity of the GPP, denoted by λ, is thus $\lambda_{\rm p}(1+p)$. For the cluster Φ_x, we call x *the cluster center*. The GPP is the union of the clusters:

$$\Phi=\bigcup_{x\in\Phi_{\rm p}}\Phi_x,$$

where the translations $\{z_x\}\in\mathbb{R}^2$, $x\in\Phi_{\rm p}$, are i.i.d. with PDF g.

In this paper, we only consider motion-invariant (isotropic and stationary) point processes, so $g(x)$ only depends on $\|x\|$, and we define the radial PDF $f_u:\mathbb{R}^+\to\mathbb{R}^+$ by $f_u(\|x\|)\triangleq g(x)$.

The generalized GPP was first introduced by Newman in [21]. Newman named the point process "Gauss-Poisson" due to its property that it is completely characterized by its first- and second-order statistics (i.e., intensity and two-point correlation function). In contrast, the stationary PPP is characterized only by its intensity. As such, the generalized GPP is a natural generalization of the PPP that retains some of its simplicity. In the following subsection, we discuss some of its pertinent properties.

B. Properties

The second factorial moment measure $\alpha^{(2)}$ [2, Def. 6.4] and the second moment density $\rho^{(2)}$ [2, Def. 6.5] of a point process are related by

$$\alpha^{(2)}(A\times B)\triangleq\mathbb{E}\Big(\sum_{x,y\in\Phi}^{\neq}\mathbf{1}_A(x)\mathbf{1}_B(y)\Big)=\int_{A\times B}\rho^{(2)}(x,y)\mathrm{d}x\mathrm{d}y,$$

where A,B are two compact subsets of $\mathbb{R}^2$ and the $\neq$ symbol indicates that the sum is taken only over distinct point pairs. The second moment density is an important statistic that describes the pairwise correlation of a point process. For the PPP, $\rho^{(2)}(x,y)=\lambda^2$, since points are independent. If $\rho^{(2)}(x,y)>\lambda^2$, it is likely that Φ has a point at y, if there is a point of Φ located at x.

Since the generalized GPP is motion-invariant, $\rho^{(2)}(x,y)$ only depends on $\|x-y\|$. So we define $\rho^{(2)}_{\rm mi}\colon\mathbb{R}^+\to\mathbb{R}^+$, such that $\rho^{(2)}_{\rm mi}(\|x-y\|)\equiv\rho^{(2)}(x,y)$, for all $x,y\in\mathbb{R}^2$. Without ambiguity, we also call $\rho^{(2)}_{\rm mi}$ the second moment density. For the GPP, an expression for $\rho^{(2)}_{\rm mi}$ is given in the following lemma.

Lemma 1. *The second moment density $\rho^{(2)}_{\rm mi}(r)$ of the generalized GPP is*

$$\rho^{(2)}_{\rm mi}(r)=\lambda^2+2p\lambda_{\rm p}f_u(r). \tag{2}$$

Proof: For any compact $A,B\subset\mathbb{R}^2$, the second moment measure is

$$\begin{aligned}\int_A\int_B\rho^{(2)}(x,y)\mathrm{d}x\mathrm{d}y&=\int_A\int_B\big(\lambda^2+p\lambda_{\rm p}g(y-x)\\&\quad+p\lambda_{\rm p}g(x-y)\big)\mathrm{d}x\mathrm{d}y \qquad (3)\\&=\int_A\int_B\big(\lambda^2+2p\lambda_{\rm p}g(y-x)\big)\mathrm{d}x\mathrm{d}y. \qquad (4)\end{aligned}$$

For the right hand side of (3), inside the integral, λ^2 is due to pairs of points in different clusters, $p\lambda_{\rm p}g(y-x)$ is due to the pair (x,y) of points in the same cluster, where $x\in A$ is the cluster center and $y\in B$ is the other point of the cluster, and $p\lambda_{\rm p}g(x-y)$ is from the pair (x,y) of points in the same cluster, where y is the cluster center and x is the other point.

Since A,B are arbitrary compact sets, we have that for any $x,y\in\mathbb{R}^2$,

$$\rho^{(2)}(x,y)=\lambda^2+2p\lambda_{\rm p}g(y-x), \tag{5}$$

and it follows that for any $r\in\mathbb{R}^+$, $\rho^{(2)}_{\rm mi}(r)=\lambda^2+2p\lambda_{\rm p}f_u(r)$. ∎

According to Lemma 1, $\rho^{(2)}_{\rm mi}(r)$ "inherits" the properties of $f_u(r)$, since $\rho^{(2)}_{\rm mi}(r)-\lambda^2\propto f_u(r)$. Indeed, defining the two-point correlation function as

$$\xi(r)\triangleq\frac{\rho^{(2)}_{\rm mi}(r)}{\lambda^2}-1, \tag{6}$$

we have

$$\xi(r)=\frac{2p}{\lambda(1+p)}f_u(r). \tag{7}$$

Let $D\triangleq\frac{2p}{\lambda(1+p)}$. Since $\int_{\mathbb{R}^2}f_u(\|x\|)\mathrm{d}x=1$, we have $\int_{\mathbb{R}^2}\xi(\|x\|)\mathrm{d}x=D$. Given the intensity λ and the two-point correlation function $\xi(r)$, we obtain for the generalized GPP

$$f_u(r)=\frac{\xi(r)}{D}, \tag{8}$$

$$p=\frac{\lambda D}{2-\lambda D}, \tag{9}$$

$$\lambda_{\rm p}=\lambda\Big(1-\frac{\lambda D}{2}\Big). \tag{10}$$

Thus, the generalized GPP is completely defined by its first-order statistic λ and its second-order statistic $\xi(r)$ (or $\rho^{(2)}_{\rm mi}(r)$). Note that (8), (9) and (10) have also been derived in [9] using a different method.

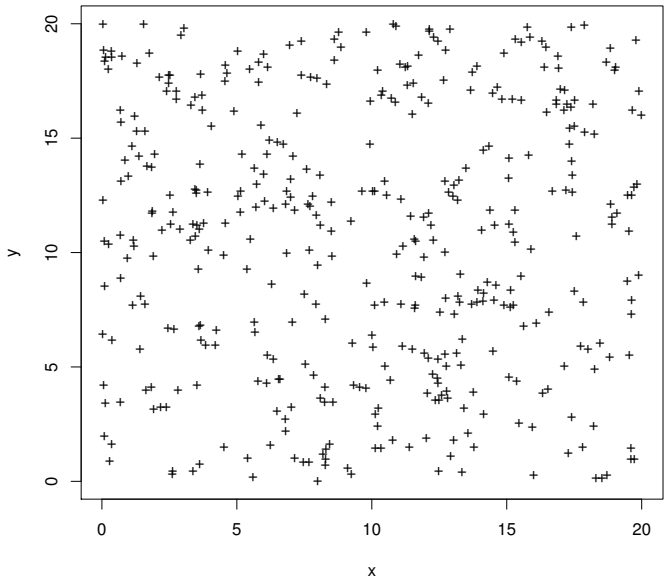

Fig. 2. The illustration of the point set we consider for the GPP fitting. It is a realization of the PHP with $\lambda_1 = 0.8825$, $\lambda_2 = 2$ and $r = 0.5$.

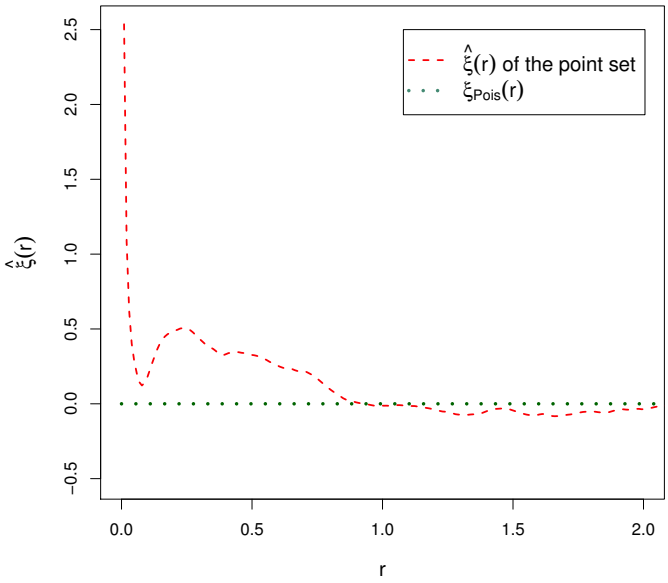

Fig. 3. The estimated two-point correlation function $\hat{\xi}(r)$ of the point set and the two-point correlation function $\xi_{\text{Pois}}(r)$ of the PPP.

Since $f_u(r) \geq 0$ for all $r \in \mathbb{R}^+$ and $\int_{\mathbb{R}^2} f_u(\|x\|)\mathrm{d}x = 1$, by (7), we have two constraints for $\xi(r)$, namely

$$\xi(r) \geq 0, \quad \forall r \in \mathbb{R}^+, \tag{11}$$

$$\lambda \int_{\mathbb{R}^2} \xi(\|x\|)\mathrm{d}x = \frac{2p}{1+p} \leq 1. \tag{12}$$

Herein, (11) indicates that the GPP is a clustered point process, and (12) implies that next to a point of the process, at most one other point in excess of the Poisson distributed points can be present. Given λ and $\xi(r)$ that statisfy the two constraints, the generalized GPP is well defined.

C. GPP Model Fitting

Given λ and $\xi(r)$, which satisfy (11) and (12), there is a generalized GPP. In this subsection, we introduce the GPP model fitting given a point set. The basic idea is that, given a point set, we first estimate its intensity $\hat{\lambda}$ and the two-point correlation function $\hat{\xi}(r)$ and then fit the generalized GPP with λ and $\xi(r)$ to the point set by letting $\lambda = \hat{\lambda}$ and $\xi(r) = \hat{\xi}(r)$. The goodness-of-fit is evaluated by comparing the nearest-neighbor distance function $G(r)$ [2, Def. 2.39].

The point set we use for fitting in this subsection is drawn from a realization of the Poisson hole process (PHP). Recently, as a class of clustered point process, the PHP has drawn much attention for its application to model some emerging types of networks. For example, in [22], the PHP is used to model active secondary users in a cognitive network, who are outside the primary user exclusion regions; in [23], the PHP is used to model the device-to-device (D2D) transmitters in D2D networks where exclusion zones are introduced by interference management. A shortcoming of the PHP is that it is not very tractable; as a result, it would benefit from being approximated using a simpler point process, such as the GPP.

The PHP is a Cox process that has been defined in [2, Example 3.7]. Let $\Phi_1, \Phi_2 \subset \mathbb{R}^2$ be independent uniform PPPs of intensities λ_1 and λ_2. Further let $\Xi_r \triangleq \bigcup\{b(x,r) : x \in \Phi_1\}$ be the unions of all disks of radius r centered at a point of Φ_1. The PHP is $\Phi = \{x \in \Phi_2 : x \notin \Xi_r\} = \Phi_2 \setminus \Xi_r$, i.e., each point in Φ_1 carves out a hole of radius r from Φ_2.

As is illustrated in Fig. 2, the point set we use for fitting is generated on a 20×20 window from the PHP with $\lambda_1 = 0.8825$, $\lambda_2 = 2$ and $r = 0.5$. The intensity of the PHP is $\lambda = \lambda_2 \exp(-\lambda_1 \pi r^2) = 1$. The estimated intensity of the point set is $\hat{\lambda} = 1.06$. To estimate the two-point correlation function, we use the function 'pcf' of the package "spatstat" in the software "R". Fig. 3 shows the estimated two-point correlation function $\hat{\xi}(r)$. We observe that $\hat{\xi}(r)$ vanishes for $r > 1$, i.e., $\hat{\xi}(r) \approx 0$, for $r > 1/\sqrt{\hat{\lambda}}$, which means that if the distance between two points is larger than twice the mean nearest-neighbor distance of the PPP with the same intensity[2], the two points are likely to be uncorrelated. To apply the generalized GPP for modeling fitting, we let $\lambda = \hat{\lambda}$ and make the approximation of $\xi(r)$ that

$$\xi(r) = \begin{cases} \max\{0, \hat{\xi}(r)\}, & \text{for } r \in \left(0, 1/\sqrt{\hat{\lambda}}\right], \\ 0, & \text{otherwise.} \end{cases} \tag{13}$$

Denote the PDF of the inter-point distance in the two-point cluster as $\hat{f}_u$. We have $\hat{f}_u(r) = 2\pi r f_u(r)$. By (8), $\hat{f}_u$ of the fitted GPP is obtained and shown in Fig. 4. By (9) and (10), we have $p = 0.460$ and $\lambda_{\text{p}} = 0.726$.

The two-point correlation functions of the point set and the fitted generalized GPP are shown in Fig. 5. The estimated two-point correlation functions of 99 realizations of the fitted generalized GPP are also illustrated. We observe that there is only a small gap between their average and $\hat{\xi}(r)$ of the point set for $r < 0.3$, and their envelope fully contains $\hat{\xi}(r)$

[2]The nearest-neighbor distance distribution $G(r)$ of the PPP of intensity λ is $G(r) = 1 - e^{-\lambda\pi r^2}$. Thus the mean nearest-neighbor distance $\overline{\text{NN}} = \int_0^\infty 2\lambda\pi r^2 e^{-\lambda\pi r^2}\mathrm{d}r = \frac{1}{2\sqrt{\lambda}}$.

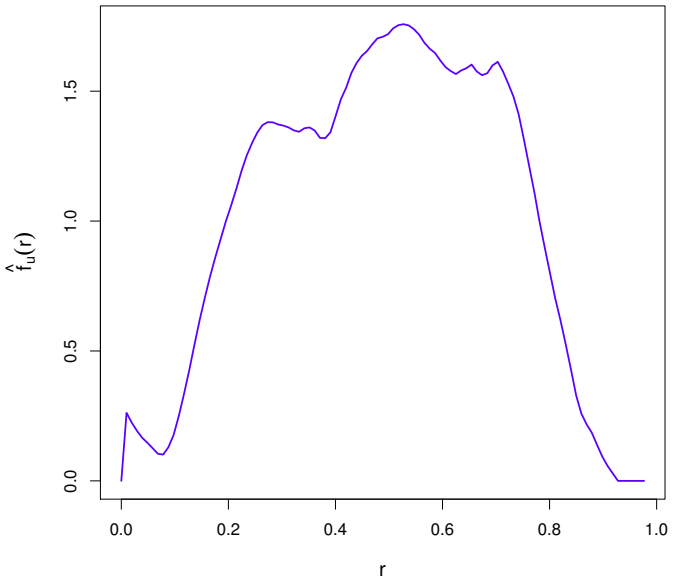

Fig. 4. The PDF $\hat{f}_u(r)$ of the distance between the two points in the same cluster for the fitted generalized GPP.

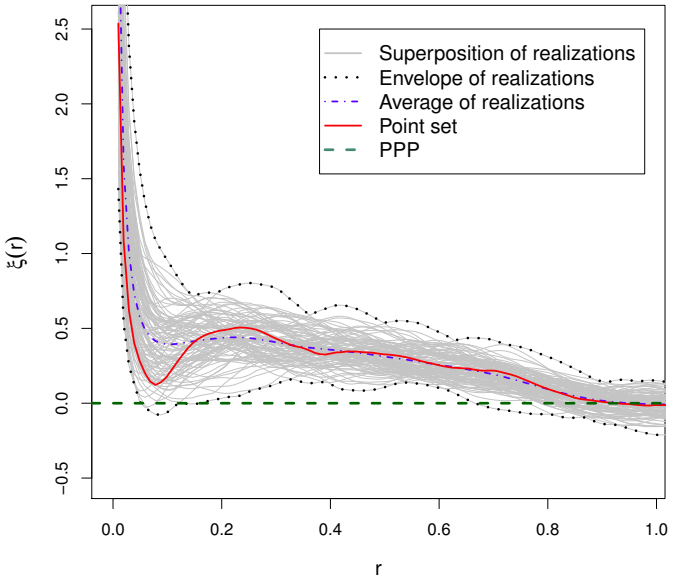

Fig. 5. The two-point correlation functions $\xi(r)$ of the data (solid curve) and 99 realizations of the fitted generalized GPP (grey curves). The dotted curve are the pointwise maximum and minimum of $\xi(r)$ of the 99 realizations. The dash-dotted curve is the average value of $\xi(r)$ of the 99 realizations. The dashed curve is the theoretical curve of the PPP.

of the point set, which implies that the approximation by (13) provides a very good match within the r range $\left[0, 1/\sqrt{\hat{\lambda}}\right]$.

We next compare the G function between the point set and the fitted generalized GPP. The functions of the point set and 99 realizations of the fitted generalized GPP are given in Fig. 6. We conclude that the PPP is not suitable to describe the point set, while the fitted generalized GPP is a good model for the point set, since the functions of the point set fall into the range of the functions of the fitted generalized GPP's 99 realizations.

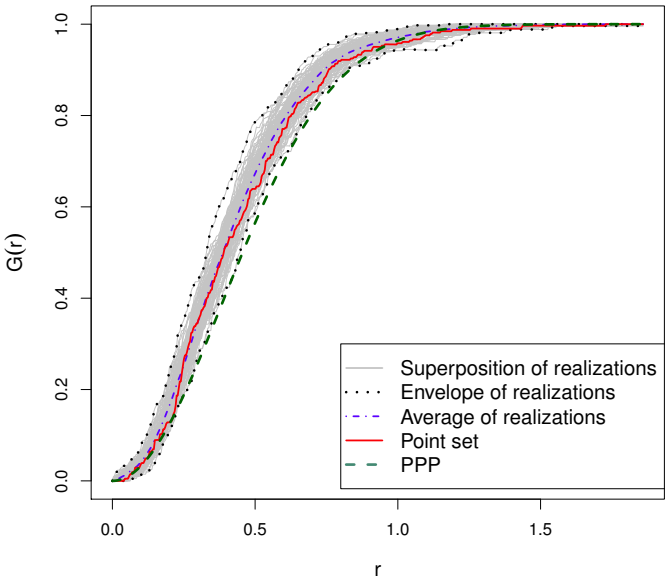

Fig. 6. The nearest-neighbor distance distribution functions $G(r)$ of the data (solid curve) and 99 realizations of the fitted generalized GPP (grey curves). The dotted curve are the pointwise maximum and minimum of $G(r)$ of the 99 realizations. The dash-dotted curve is the average value of $G(r)$ of the 99 realizations. The dashed curve is the theoretical curve of the PPP.

III. System Models

We model the locations of the transmitters as a generalized GPP on $\mathbb{R}^2$. As a special case, the modeling using the standard GPP has been considered in our prior work [1]. Our analysis is focused on the typical receiver located at the origin o with desired transmitter at $x_0 = (b, 0)$ with $b \neq 0$.

We adopt a path loss model $\ell(x) = \|x\|^{-\alpha}$, where $x \in \mathbb{R}^2$ and $\alpha > 2$, and assume the power fading coefficients to be spatially independent with exponential distribution of unit mean (i.e., Rayleigh fading). Denote by h_x the power fading coefficient between the transmitter x and the receiver at o. We set all transmit powers to unity and focus on the interference-limited regime, thus omitting the thermal noise.

A. Basic Model

The desired transmitter x_0 is separate from the GPP and all points in the GPP are interferers. The SIR at the receiver located at the origin o is

$$\mathrm{SIR} = \frac{h_0 b^{-\alpha}}{\sum_{x \in \Phi} h_x \|x\|^{-\alpha}}, \tag{14}$$

where h_0 is the power fading coefficient between the desired transmitter and the receiver.

B. Non-cooperative Model

In this case, the desired transmitter x_0 is taken from the GPP and $b = \|x_0\|$. All other points in the GPP are interferers. Therefore, there is an interferer at distance u of the desired transmitter with probability $\frac{2p}{1+p}$, since the probability that x_0

belongs to a one-point cluster is $\frac{(1-p)\lambda_{\rm p}}{\lambda_{\rm p}+p\lambda_{\rm p}}=\frac{1-p}{1+p}$, and the SIR at the receiver is

$$\mathrm{SIR}=\frac{h_{x_0}b^{-\alpha}}{\sum_{x\in\Phi\setminus\{x_0\}}h_x\|x\|^{-\alpha}}. \tag{15}$$

C. Cooperative Model 1

In this case, the desired transmitter x_0 is taken from a cluster Φ_0 in the GPP, and if there is another point in Φ_0, it acts as a cooperator. Unlike the cooperation model in [19], where the cooperative base stations are selected based on the received signal strength measurements, in our model, we assume that the cooperative pair consists of the transmitters in the same cluster and that they share the information including the data that needs to be transmitted. We assume that if there is a cooperator, the transmitters adopt non-coherent JT and at the receiver, the useful signals are combined by accumulating their powers, a scheme known as cyclic delay diversity for single-frequency networks using orthogonal frequency division multiplexing (OFDM) as is shown in [19]. In this way, the receiver is served by both transmitters in a cluster, and all points from other clusters of the GPP act as interferers. The SIR at the receiver is

$$\mathrm{SIR}=\frac{\sum_{x\in\Phi_0}h_x\|x\|^{-\alpha}}{\sum_{x\in\Phi\setminus\Phi_0}h_x\|x\|^{-\alpha}}. \tag{16}$$

D. Cooperative Model 2

In this case, same as the cooperative model 1, the desired transmitter x_0 is taken from a cluster Φ_0 in the GPP, and if Φ_0 has two points, the other point acts as a cooperator. But different from the cooperative model 1, if there exists a cooperator, the signals from the two cooperative transmitters are not combined at the receiver by accumulating their powers but they add up in amplitude. The received signal at the typical receiver is expressed as

$$Y_{ro}=\sum_{x\in\Phi_0}\tilde{h}_x\|x\|^{-\alpha/2}X_{to}+\sum_{z\in\Phi\setminus\Phi_0}\tilde{h}_z\|z\|^{-\alpha/2}X_z, \tag{17}$$

where $\tilde{h}_x$ are the fading coefficients and are i.i.d. complex Gaussian distributed random variables with mean 0 and variance 1, X_{to} is the signal transmitted by the desired (cooperative) transmitters of the typical receiver, and X_z is the signal transmitted by the transmitter at z. X_{to} and X_z are independent random variables with mean 0 and variance 1. The first term is the desired signal, while the second term is the interfering signal. The desired received signal power at o is

$$P_r=\Big|\sum_{x\in\Phi_0}\tilde{h}_x\|x\|^{-\alpha/2}\Big|^2. \tag{18}$$

So P_r is exponentially distributed with mean $\sum_{x\in\Phi_0}\|x\|^{-\alpha}$ (i.e., Rayleigh fading). Note that in the interference signal, if two transmitters belong to one cluster, they transmit the same signal. So the interference power at o is given by

$$I_o=\sum_{y\in\Phi_{\rm p}\setminus\Phi_0}\Big|\sum_{x\in\Phi_y}\tilde{h}_x\|x\|^{-\alpha/2}\Big|^2. \tag{19}$$

where $\{\Phi_y\}$ are the clusters of the GPP and y is the cluster center of Φ_y.

Therefore, the SIR at the receiver o is

$$\mathrm{SIR}=\frac{\Big|\sum_{x\in\Phi_0}\tilde{h}_x\|x\|^{-\alpha/2}\Big|^2}{\sum_{y\in\Phi_{\rm p}\setminus\Phi_0}\Big|\sum_{x\in\Phi_y}\tilde{h}_x\|x\|^{-\alpha/2}\Big|^2}. \tag{20}$$

IV. SIR Distribution

We assume that the receiver can decode successfully if its SIR exceeds a threshold θ. The interference is denoted by I, which is the denominator in (14), (15), (16) and (20). In this section, we derive the complementary cumulative distribution function (CCDF) of the SIR distributions (or the transmission success probabilities) for the four models.

A. Basic Model

Lemma 2. *Let $v:\mathbb{R}^2\mapsto[0,1]$ be a measurable function such that $1-v$ has bounded support. The probability generating functional (PGFL) of the GPP is*

$$G[v]=\exp\bigg(\lambda_{\rm p}\int_{\mathbb{R}^2}\Big[(1-p)v(x)+pv(x)\int_{\mathbb{R}^2}v(x+z)f_u(\|z\|)\mathrm{d}z-1\Big]\mathrm{d}x\bigg). \tag{21}$$

Proof: The PGFL of a Poisson cluster process is

$$G^{\rm PCP}[v]=\exp\Big(\lambda_{\rm p}\int_{\mathbb{R}^2}(G_0^{[x]}[v]-1)\mathrm{d}x\Big), \tag{22}$$

where $G_0^{[x]}[v]$ is the PGFL of the cluster $\Phi^{[x]}$ that is centered at x, given by $G_0^{[x]}[v]=\mathbb{E}\big(\prod_{y\in\Phi^{[x]}}v(y)\big)$ [2, Cor. 4.12].

According to the definition of the generalized GPP, we have

$$G_0^{[x]}[v]=(1-p)v(x)+p\int_{\mathbb{R}^2}v(x)v(x+z)f_u(\|z\|)\mathrm{d}z. \tag{23}$$

Substituting (23) into (22), we obtain (21). ■

Theorem 1. *In the basic model, the SIR distribution is the Laplace transform of the interference I at θb^α, i.e.,*

$$P_{\rm s}(\theta,b,\lambda_{\rm p},\alpha,p)=\mathcal{L}_I(\theta b^\alpha), \tag{24}$$

where

$$\mathcal{L}_I(s)=\exp\bigg(2\pi\lambda_{\rm p}\int_0^\infty\bigg(\frac{1-p}{1+sr^{-\alpha}}+\frac{p}{1+sr^{-\alpha}}\cdot\int_0^\infty\int_0^{2\pi}\frac{1}{1+s(r^2+\tau^2+2r\tau\cos\psi)^{-\alpha/2}}\mathrm{d}\psi f_u(\tau)\tau\mathrm{d}\tau-1\bigg)r\mathrm{d}r\bigg). \tag{25}$$

Proof: The SIR distribution $P_{\rm s}$ is

$$P_{\rm s}(\theta,b,\lambda_{\rm p},\alpha,p)=\mathbb{P}\bigg(\frac{h_0b^{-\alpha}}{I}>\theta\bigg)\overset{(a)}{=}\mathcal{L}_I(\theta b^\alpha), \tag{26}$$

where (a) follows because $h_0 \sim \exp(1)$. The Laplace transform of I is derived from the PGFL as follows:

$$\begin{aligned}\mathcal{L}_I(s) &= \mathbb{E}_{\Phi,\{h\}}\Big(\exp\Big(-\sum_{x\in\Phi} sh_x\|x\|^{-\alpha}\Big)\Big)\\ &= \mathbb{E}_{\Phi}\Big(\prod_{x\in\Phi}\mathbb{E}_h\big(\exp(-sh\|x\|^{-\alpha})\big)\Big)\\ &= \exp\Big(\lambda_{\rm p}\int_{\mathbb{R}^2}\Big[(1-p)v(x)+pv(x)\\ &\quad\cdot\int_{\mathbb{R}^2} v(x+z)f_u(\|z\|)\mathrm{d}z-1\Big]\mathrm{d}x\Big),\end{aligned} \tag{27}$$

where

$$v(x) = \mathbb{E}_h\big(\exp(-sh\|x\|^{-\alpha})\big) = \frac{1}{1+s\|x\|^{-\alpha}}. \tag{28}$$

Substituting (28) into (27), we obtain (25). ∎

The SIR distribution can be bounded in closed form for the standard GPP with $u=1$ and $\alpha=4$.

Corollary 1. *For the standard GPP with $u=1$ and $\alpha=4$, the SIR distribution has upper and lower bounds in closed form, as follows:*

$$P_{\rm s}(\theta,b,\lambda_{\rm p},4,p) \le \exp\Big(-\frac{\pi^2}{2}\lambda_{\rm p}(1-p)\sqrt{s}+\lambda_{\rm p}pW_{\rm u}(s)\Big),$$

and

$$P_{\rm s}(\theta,b,\lambda_{\rm p},4,p) \ge \exp\Big(-\frac{\pi^2}{2}\lambda_{\rm p}(1-p)\sqrt{s}+\lambda_{\rm p}pW_{\rm l}(s)\Big),$$

where $s=\theta b^4$,

$$\begin{aligned}W_{\rm u}(s) &= \frac{\pi\sqrt{s}}{4(9s^2+40s+16)}\Big(8s^{\frac{3}{2}}\ln\frac{s}{s+4}+(-3s^2+24s\\ &\quad+16)\arctan\frac{2}{\sqrt{s}}-\pi(\frac{21}{2}s^2+48s+24)\Big)+\frac{\pi\sqrt{s}}{2(4s+1)}\\ &\quad\cdot\Big(s^{\frac{3}{2}}\ln\frac{s}{s+1}+(3s+1)(\arctan\frac{1}{\sqrt{s}}-\pi)\Big),\end{aligned} \tag{29}$$

and

$$\begin{aligned}W_{\rm l}(s) &= -\frac{\pi^2\sqrt{s}}{4}-\frac{\pi s^{\frac{1}{4}}}{8}\Big(2\sqrt{2}\pi-\sqrt{2}\ln\frac{1+\sqrt{s}-\sqrt{2}s^{\frac{1}{4}}}{1+\sqrt{s}+\sqrt{2}s^{\frac{1}{4}}}\\ &\quad-2(\sqrt{2}+2s^{\frac{1}{4}})\arctan\frac{-\sqrt{2}-s^{\frac{1}{4}}}{s^{\frac{1}{4}}}-2(\sqrt{2}-2s^{\frac{1}{4}})\\ &\quad\cdot\arctan\frac{-\sqrt{2}+s^{\frac{1}{4}}}{s^{\frac{1}{4}}}\Big)+\frac{2\pi s^{\frac{3}{2}}+\pi\sqrt{s}}{2(4s+1)}\arctan\frac{1}{\sqrt{s}}\\ &\quad+\frac{\pi s^2}{4s+1}\ln\frac{s}{s+1}-\frac{2\pi^2 s^{\frac{3}{2}}+\pi^2\sqrt{s}}{2(4s+1)}.\end{aligned} \tag{30}$$

Proof: See Appendix A. ∎

As $b\to 0$, we have $W_{\rm u}\to 0$ and $W_{\rm l}\to 0$, and thus the gap between $W_{\rm u}$ and $W_{\rm l}$ vanishes.

The following corollary gives the SIR distribution in the asymptotic regime $u\to 0$ for the standard GPP.

Corollary 2. *In the basic model, for the standard GPP, the SIR distribution in the asymptotic regime $u\to 0$ is equal to the Laplace transform of the interference I_0 at θb^α, i.e.,*

$$P_{\rm s}(\theta,b,\lambda_{\rm p},\alpha,p) = \mathcal{L}_{I_0}(s), \tag{31}$$

where $s=\theta b^\alpha$,

$$\mathcal{L}_{I_0}(s) = \exp\Big(-\frac{\pi\lambda_{\rm p}s^\delta}{\operatorname{sinc}\delta}(1+p\delta)\Big), \tag{32}$$

and $\delta \triangleq \frac{2}{\alpha}$.

Proof: For the asymptotic regime $u\to 0$, the two points in any two-point cluster tend to be located at the same position. Let $\Phi_1\subset\Phi_{\rm p}$ be the set of parent points of the clusters with only one point in the GPP and $\Phi_2=\Phi_{\rm p}\backslash\Phi_1$ be the set of parent points of the clusters with co-located two points in the GPP. Let $I_1=\sum_{x\in\Phi_1}h_x\|x\|^{-\alpha}$ and $I_2=\sum_{x\in\Phi_2}(h_{x,1}+h_{x,2})\|x\|^{-\alpha}$ be the interference from Φ_1 and Φ_2 respectively, where $h_{x,1}$ and $h_{x,2}$ are the power fading coefficients between the two transmitters co-located at x and the typical receiver. The Laplace transform of the interference is then given by

$$\begin{aligned}\mathcal{L}_{I_0}(s) &= \mathbb{E}\Big(\exp\big(-sI_1-sI_2\big)\Big)\\ &= \mathbb{E}_{\Phi_1}\Big(\prod_{x\in\Phi_1}\mathbb{E}_h\big(\exp(-sh\|x\|^{-\alpha})\big)\Big)\\ &\quad\cdot\mathbb{E}_{\Phi_2}\Big(\prod_{x\in\Phi_2}\mathbb{E}_{h_{x,1},h_{x,2}}\big(\exp(-s(h_{x,1}+h_{x,2})\|x\|^{-\alpha})\big)\Big)\\ &= \mathbb{E}_{\Phi_1}\Big(\prod_{x\in\Phi_1}\frac{1}{1+s\|x\|^{-\alpha}}\Big)\mathbb{E}_{\Phi_2}\Big(\prod_{x\in\Phi_2}\frac{1}{(1+s\|x\|^{-\alpha})^2}\Big)\\ &= \exp\Big(-\lambda_{\rm p}\int_{R^2}\frac{(1+p+s\|x\|^{-\alpha})s\|x\|^{-\alpha}}{(1+s\|x\|^{-\alpha})^2}\mathrm{d}x\Big)\\ &= \exp\Big(-\frac{\delta\pi^2\lambda_{\rm p}s^\delta}{\sin(\pi\delta)}(1+p\delta)\Big).\end{aligned} \tag{33}$$

From (26), we get the SIR distribution for the GPP in the limit of $u\to 0$. ∎

B. Non-cooperative Model

Lemma 3. *Conditioned on a point of the generalized GPP being located at y, the conditional PGFL of the GPP excluding y is*

$$G_y^!(v] = G[v]\Big(\frac{1-p}{1+p}+\frac{2p}{1+p}\int_{\mathbb{R}^2}v(y+z)f_u(\|z\|)\mathrm{d}z\Big).$$

Proof: Denote the points in the cluster which contains the desired transmitter y as Φ_0 and all points in other clusters as $\Phi_{\rm c}=\Phi\backslash\Phi_0$. From Slivnyak's theorem [2], conditioning on Φ_0 does not change the distribution of the other clusters, and the distribution of the points excluding Φ_0 remains the same as the original GPP Φ. So, the conditional PGFL excluding y is

$$\begin{aligned}G_y^!(v] &= \mathbb{E}\Big(\prod_{x\in(\Phi_{\rm c}\bigcup\Phi_0)\backslash\{y\}}v(x)\Big)\\ &= \mathbb{E}\Big(\prod_{x\in\Phi}v(x)\Big)\mathbb{E}\Big(\prod_{x\in\Phi_0\backslash\{y\}}v(x)\Big)\\ &\overset{(a)}{=} G[v]\Big(\frac{1-p}{1+p}+\frac{2p}{1+p}\int_{\mathbb{R}^2}v(y+z)f_u(\|z\|)\mathrm{d}z\Big),\end{aligned}$$

where (a) follows since the probability that y belongs to a one-point cluster is $\frac{(1-p)\lambda_{\rm p}}{\lambda_{\rm p}+p\lambda_{\rm p}}=\frac{1-p}{1+p}$. ∎

Theorem 2. *In the non-cooperative model, the SIR distribution is the Laplace transform of the interference I at θb^α*

$$P_{\rm s}(\theta,b,\lambda_{\rm p},\alpha,p)=\bar{\mathcal{L}}_I(s), \tag{34}$$

where $s=\theta b^\alpha$ and

$$\bar{\mathcal{L}}_I(s)=\mathcal{L}_I(s)\cdot\bigg(\frac{1-p}{1+p}+\frac{2p}{1+p}\cdot\int_0^\infty\int_0^{2\pi}\frac{1}{1+s(b^2+\tau^2+2b\tau\cos\psi)^{-\alpha/2}}{\rm d}\psi f_u(\tau)\tau{\rm d}\tau\bigg).$$

Proof: The proof is similar to that of Theorem 1, with the conditional PGFL $G_y^!{}[v]$ instead of $G[v]$. ∎

Similar to the basic model, $P_{\rm s}(\theta,b,\lambda_{\rm p},\alpha,p)$ is not in closed form. For the standard GPP with $u=1$ and $\alpha=4$, however, closed-form lower and upper bounds are available.

Corollary 3. *For the standard GPP with $u=1$ and $\alpha=4$, the SIR distribution has upper and lower bounds in closed form, as follows:*

$$P_{\rm s}(\theta,b,\lambda_{\rm p},4,p)\le\exp\bigg(-\frac{\pi^2}{2}\lambda_{\rm p}(1-p)\sqrt{s}+\lambda_{\rm p}pW_{\rm u}(s)\bigg)\cdot\bigg(\frac{1-p}{1+p}+\frac{p}{1+p}\Big(\frac{1}{1+s(b^2+1+2b)^{-2}}+\frac{1}{1+s(b^2+1)^{-2}}\Big)\bigg),$$

and

$$P_{\rm s}(\theta,b,\lambda_{\rm p},4,p)\ge\exp\bigg(-\frac{\pi^2}{2}\lambda_{\rm p}(1-p)\sqrt{s}+\lambda_{\rm p}pW_{\rm l}(s)\bigg)\cdot\bigg(\frac{1-p}{1+p}+\frac{p}{1+p}\Big(\frac{1}{1+s(b^2+1-2b)^{-2}}+\frac{1}{1+s(b^2+1)^{-2}}\Big)\bigg),$$

where $s=\theta b^4$.

Proof: See Appendix B. ∎

The SIR distribution in the asymptotic regime $u\to 0$ for the standard GPP is given by the following corollary.

Corollary 4. *In the non-cooperative model, for the standard GPP, the SIR distribution as $u\to 0$ is equal to the Laplace transform of the interference I_0 at θb^α, i.e.,*

$$P_{\rm s}(\theta,b,\lambda_{\rm p},\alpha,p)=\bar{\mathcal{L}}_{I_0}(s), \tag{35}$$

where $s=\theta b^\alpha$ and

$$\bar{\mathcal{L}}_{I_0}(s)=\frac{(1+p)b^\alpha+(1-p)s}{(1+p)(b^\alpha+s)}\exp\bigg(-\frac{\pi\lambda_{\rm p}s^\delta}{\operatorname{sinc}\delta}(1+p\delta)\bigg).$$

Proof: The proof follows the same reasoning as that of Corollary 2 except for the conditional PGFL of the GPP as $u\to 0$. ∎

Compared with the corresponding result for the basic model, the result for the non-cooperative model has an extra factor $\frac{(1+p)b^\alpha+(1-p)s}{(1+p)(b^\alpha+s)}$. This factor is a result of the extra factor of the conditional PGFL of the GPP, compared with the PGFL of the GPP.

C. Cooperative Model 1

In this cooperative model, the cooperator transmits the same information as the desired transmitter simultaneously. In this case, the received power, denoted by $P_{\rm sum}$, is the sum of the received signal powers from the desired transmitter and the cooperator, i.e.,

$$P_{\rm sum}=\begin{cases}hb^{-\alpha} & \text{w.p. } \frac{1-p}{1+p},\\ h_1b^{-\alpha}+h_2c^{-\alpha} & \text{w.p. } \frac{2p}{1+p},\end{cases} \tag{36}$$

where $h,h_1,h_2\sim\exp(1)$ are mutually independent, $c=\|x_0+z_c\|$, and $z_c\in\mathbb{R}^2$ is a random point with PDF f_u.

The exponential distribution has the property that if $h\sim\exp(1)$, then $lh\sim\exp(1/l)$, for $l>0$. Thus, conditioned on c, for the case where $P_{\rm sum}=h_1b^{-\alpha}$, $P_{\rm sum}\sim\exp(b^\alpha)$; for the case where $P_{\rm sum}=h_1b^{-\alpha}+h_2c^{-\alpha}$, if $b\neq c$, $P_{\rm sum}$ follows the hypoexponential distribution Hypo(b^α,c^α) and the PDF of $P_{\rm sum}$ is $f_P(x)=\frac{b^\alpha c^\alpha}{b^\alpha-c^\alpha}\big(\exp(-c^\alpha x)-\exp(-b^\alpha x)\big)$, otherwise, $P_{\rm sum}\sim$ Erlang$(2,b^\alpha)$ and $f_P(x)=b^{2\alpha}x\exp(-b^\alpha x)$.

Conditioned on $y\in\Phi_0$, the conditional PGFL $G_y^{!\Phi_0}$ of the GPP, excluding Φ_0, is

$$G_y^{!\Phi_0}[v]=G[v]. \tag{37}$$

This follows from Slivnyak's theorem.

Theorem 3. *In the cooperative model 1, the SIR distribution is*

$$P_{\rm s}(\theta,b,\lambda_{\rm p},\alpha,p)=\frac{1-p}{1+p}\mathcal{L}_I(\theta b^\alpha)+\frac{2p}{1+p}\mathbb{E}_{z_c}\big(H(\|x_0+z_c\|)\big) \tag{38}$$

where

$$H(c)\triangleq\frac{b^\alpha}{b^\alpha-c^\alpha}\mathcal{L}_I(\theta c^\alpha)-\frac{c^\alpha}{b^\alpha-c^\alpha}\mathcal{L}_I(\theta b^\alpha) \tag{39}$$

and the PDF of z_c is f_u.

Proof: The SIR at the receiver is $P_{\rm sum}/I$. We have

$$\begin{aligned}P_{\rm s}(\theta,b,\lambda_{\rm p},\alpha,p)&=\mathbb{E}_{P_{\rm sum}}\mathbb{P}\Big(\frac{P_{\rm sum}}{I}>\theta\Big)\\&=\frac{1-p}{1+p}\mathbb{P}\Big(\frac{hb^{-\alpha}}{I}>\theta\Big)\\&\quad+\frac{2p}{1+p}\mathbb{P}\Big(\frac{h_1b^{-\alpha}+h_2c^{-\alpha}}{I}>\theta\Big)\\&=\frac{1-p}{1+p}\mathcal{L}_I(\theta b^\alpha)+\frac{2p}{1+p}Q,\end{aligned} \tag{40}$$

where $Q\triangleq\mathbb{P}(\frac{h_1b^{-\alpha}+h_2c^{-\alpha}}{I}>\theta)$. Since the case of $c=b$ has a vanishing probability thus contributing zero to Q, we have $Q=\mathbb{E}_{I,c}\big(\frac{b^\alpha}{b^\alpha-c^\alpha}\exp(-\theta c^\alpha I)-\frac{c^\alpha}{b^\alpha-c^\alpha}\exp(-\theta b^\alpha I)\big)=\mathbb{E}_c\big(H(c)\big)$.

As $c=\|x_0+z_c\|$, where $z_c\in\mathbb{R}^2$ is a random point with PDF f_u, we have $Q=\mathbb{E}_{z_c}\big(H(\|x_0+z_c\|)\big)$. ∎

For the standard GPP with $u=1$ and $\alpha=4$, upper and lower bounds of the SIR distribution can be derived.

Corollary 5. *For the standard GPP with $u=1$ and $\alpha=4$ and $b\neq 1/2$, the SIR distribution has upper and lower bounds, as follows:*

$$P_{\rm s}(\theta,b,\lambda_{\rm p},4,p)\le C_1\mathcal{L}_I(\theta b^4)+C_2\mathcal{L}_I(\theta|b-1|^4), \tag{41}$$

and

$$P_{\rm s}(\theta,b,\lambda_{\rm p},4,p) \geq C_3\mathcal{L}_I(\theta b^4)+C_4\mathcal{L}_I(\theta(b+1)^4), \quad (42)$$

where $C_1=\frac{1-p}{1+p}-\frac{2p|b-1|^4}{(1+p)(b^4-|b-1|^4)}$, $C_2=\frac{2pb^4}{(1+p)(b^4-|b-1|^4)}$, $C_3=\frac{1-p}{1+p}-\frac{2p(b+1)^4}{(1+p)(b^4-(b+1)^4)}$ *and* $C_4=\frac{2pb^4}{(1+p)(b^4-(b+1)^4)}$.

Proof: See Appendix C. ∎

To get the bounds in closed form, we may apply (24) and Corollary 1 to (41) and (42). In (41), for each of the two terms $C_1\mathcal{L}_I(\theta b^4)$ and $C_2\mathcal{L}_I(\theta|b-1|^4)$, we apply the upper bound of $\mathcal{L}_I(\cdot)$, if the corresponding factor (C_1 or C_2) is larger than 0, and apply the lower bound of $\mathcal{L}_I(\cdot)$ otherwise. While in (42), for each of the two terms, we apply the lower bound of $\mathcal{L}_I(\cdot)$ if the corresponding factor is larger than 0, and apply the upper bound of $\mathcal{L}_I(\cdot)$ otherwise. Note that the upper bound becomes loose as $b\to 0.5$, as will be observed in Section V.

The SIR distribution in the asymptotic regime $u\to 0$ for the standard GPP is given by the following corollary.

Corollary 6. *In the cooperative model 1, as $u\to 0$ for the standard GPP, the SIR distribution is*

$$P_{\rm s}(\theta,b,\lambda_{\rm p},\alpha,p)=\int_{-\infty}^{\infty}\frac{(1+3p)\theta b^{\alpha}-(1+p)2j\pi\omega}{(1+p)(\theta b^{\alpha}-2j\pi\omega)^2}\cdot\exp\Big(-\frac{\pi\lambda_{\rm p}(2j\pi\omega)^{\delta}}{\operatorname{sinc}\delta}(1+p\delta)\Big)\mathrm{d}\omega. \quad (43)$$

Proof: See Appendix D. ∎

D. Cooperative Model 2

In this cooperative model, the interference signals from the same cluster can be treated as one signal, since in any cluster Φ_y with $y\in\Phi_{\rm p}\setminus\Phi_0$, the interference power is $\Big|\sum_{x\in\Phi_y}\tilde{h}_x\|x\|^{-\alpha/2}\Big|^2$, which follows the exponential distribution with mean $\sum_{x\in\Phi_y}\|x\|^{-\alpha}$. In this way, each cluster can be treated as one interferer, which follows the PPP with intensity $\lambda_{\rm p}$. Thus, the Laplace transform of the interference power I_o is given by

$$\begin{aligned}\tilde{\mathcal{L}}_{I_o}(s)&=\mathbb{E}_{\Phi,\{\tilde{h}\}}\Big(\exp\Big(-s\sum_{y\in\Phi_{\rm p}\setminus\Phi_0}\Big|\sum_{x\in\Phi_y}\tilde{h}_x\|x\|^{-\alpha/2}\Big|^2\Big)\Big)\\&=\mathbb{E}_{\Phi}\Big(\prod_{y\in\Phi_{\rm p}\setminus\Phi_0}\mathbb{E}_{\Phi_y,\{\tilde{h}\}}\big(\exp(-s\Big|\sum_{x\in\Phi_y}\tilde{h}_x\|x\|^{-\alpha/2}\Big|^2)\big)\Big)\\&=\mathbb{E}_{\Phi_p}\Big(\prod_{x\in\Phi_p}\Big((1-p)\frac{1}{1+s\|x\|^{-\alpha}}+p\int_{\mathbb{R}^2}\frac{1}{1+s(\|x\|^{-\alpha}+\|x+z\|^{-\alpha})}f_u(\|z\|)\mathrm{d}z\Big)\Big)\\&=\exp\Big(\lambda_{\rm p}\int_{\mathbb{R}^2}\Big[(1-p)\frac{1}{1+s\|x\|^{-\alpha}}+p\int_{\mathbb{R}^2}\frac{1}{1+s(\|x\|^{-\alpha}+\|x+z\|^{-\alpha})}f_u(\|z\|)\mathrm{d}z-1\Big]\mathrm{d}x\Big).\end{aligned} \quad (44)$$

Based on the expression of the Laplace transform of the interference power, we give the SIR distribution in the following theorem.

Theorem 4. *In the cooperative model 2, the SIR distribution is*

$$P_{\rm s}(\theta,b,\lambda_{\rm p},\alpha,p)=\frac{1-p}{1+p}\tilde{\mathcal{L}}_{I_o}(\theta b^{\alpha})+\frac{2p}{1+p}\int_{\mathbb{R}^2}\tilde{\mathcal{L}}_{I_o}\Big(\frac{\theta}{b^{-\alpha}+\|x_0+z\|^{-\alpha}}\Big)f_u(\|z\|)\mathrm{d}z, \quad (45)$$

where $\tilde{\mathcal{L}}_{I_o}(s)$ is given in (44).

Proof: According to the SIR expression given in (20), we have

$$\begin{aligned}P_{\rm s}(\theta,b,\lambda_{\rm p},\alpha,p)&=\mathbb{P}\Big(\frac{\Big|\sum_{x\in\Phi_0}\tilde{h}_x\|x\|^{-\alpha/2}\Big|^2}{I_o}>\theta\Big)\\&=\frac{1-p}{1+p}\mathbb{P}\Big(\frac{|\tilde{h}_{x_0}b^{-\alpha/2}|^2}{I_o}>\theta\Big)+\frac{2p}{1+p}\mathbb{P}\Big(\frac{|\tilde{h}_1b^{-\alpha/2}+\tilde{h}_2c^{-\alpha/2}|^2}{I_o}>\theta\Big)\\&=\frac{1-p}{1+p}\tilde{\mathcal{L}}_{I_o}(\theta b^{\alpha})+\frac{2p}{1+p}\mathbb{E}_c\Big[\tilde{\mathcal{L}}_{I_o}(\theta(b^{-\alpha}+c^{-\alpha})^{-1})\Big]\\&=\frac{1-p}{1+p}\tilde{\mathcal{L}}_{I_o}(\theta b^{\alpha})+\frac{2p}{1+p}\int_{\mathbb{R}^2}\tilde{\mathcal{L}}_{I_o}\Big(\frac{\theta}{b^{-\alpha}+\|x_0+z\|^{-\alpha}}\Big)f_u(\|z\|)\mathrm{d}z,\end{aligned} \quad (46)$$

where $c=\|x_0+z_c\|$, $z_c\in\mathbb{R}^2$ is a random point with PDF f_u, and $\tilde{h}_{x_0},\tilde{h}_1,\tilde{h}_2\sim\mathcal{CN}(0,1)$ are independent. ∎

The SIR distribution in the asymptotic regime $u\to 0$ for the standard GPP is given by the following corollary.

Corollary 7. *In the cooperative model 2, as $u\to 0$, the SIR distribution is*

$$P_{\rm s}(\theta,b,\lambda_{\rm p},\alpha,p)=\frac{1-p}{1+p}\exp\Big(-\frac{\pi\lambda_{\rm p}\theta^{\delta}b^2(1-p+2^{\delta}p)}{\operatorname{sinc}\delta}\Big)+\frac{2p}{1+p}\exp\Big(-\frac{\pi\lambda_{\rm p}\theta^{\delta}b^2(2^{-\delta}-2^{-\delta}p+p)}{\operatorname{sinc}\delta}\Big). \quad (47)$$

Proof: See Appendix E. ∎

It is worth noting that if $p=0$, the GPP reduces to the PPP with intensity $\lambda=\lambda_{\rm p}$. Substituting $p=0$ into either one of Theorems 1-4, we obtain the well-known result $P_{\rm s}(\theta)=\exp\big(-\pi\lambda_{\rm p}\theta^{\delta}b^2\Gamma(1+\delta)\Gamma(1-\delta)\big)$, see, e.g., [2, Ch. 5.2].

V. Numerical results

We consider all system models we analyzed and show the numerical results. The numerical results are obtained from the analytical results we have derived.

A. Deterministic u (Standard GPP)

Fig. 7 shows the SIR distribution and the closed-form bounds of the basic model as a function of the distance between the receiver and the desired transmitter. We observe that the upper bounds are satisfactorily tight for the basic model.

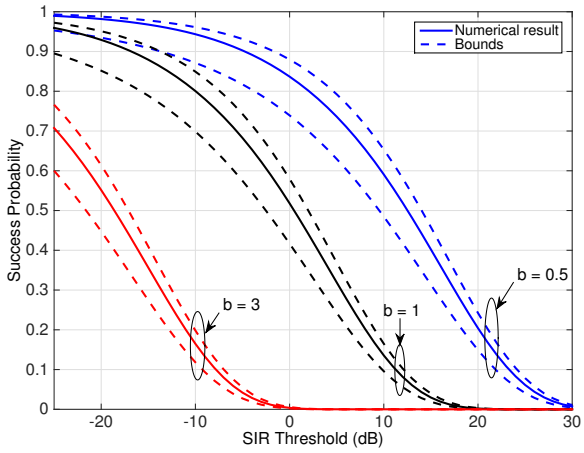

Fig. 7. The SIR distribution and the closed-form bounds with different distances between the receiver and the desired transmitter for the basic model ($\lambda_{\rm p} = 0.1, p = 0.5, \alpha = 4, u = 1$).

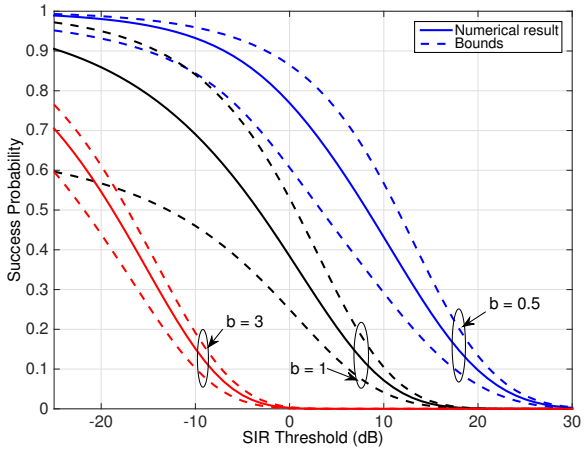

Fig. 8. The SIR distribution and the closed-form bounds with different distances between the receiver and the desired transmitter for the non-cooperative model ($\lambda_{\rm p} = 0.1, p = 0.5, \alpha = 4, u = 1$).

Fig. 8 shows the SIR distribution and the closed-form bounds of the non-cooperative model as a function of the distance between the receiver and the desired transmitter. We observe that the upper bounds are tight for both large and small values of b. However, when b approaches u, the bounds become loose, since if the cluster containing the desired transmitter has another transmitter z_0, we use the bounds for the distance $d_{\rm zr}$ from z_0 to the receiver that $\sqrt{b^2+u^2} < d_{\rm zr} < b+u$ with probability 0.5 and $|b-u| < d_{\rm zr} < \sqrt{b^2+u^2}$ with probability 0.5.

Fig. 9 shows the SIR distribution and the closed-form bounds of the cooperative model 1 as a function of the distance between the receiver and the desired transmitter. We also observe that the bounds are tight for both large and small values of b, while they become loose when b is close to u. The SIR distributions for the cooperative model 2 are also shown in Fig. 9. Interestingly, they are approximately the same as those for the cooperative model 1. So under our system

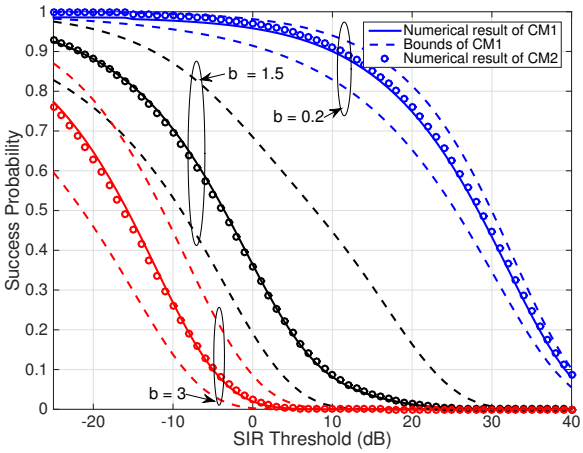

Fig. 9. The SIR distribution and the closed-form bounds with different distances between the receiver and the desired transmitter for the cooperative model 1 (CM1) and the SIR distribution for the cooperative model 2 (CM2). ($\lambda_{\rm p} = 0.1, p = 0.5, \alpha = 4, u = 1.$)

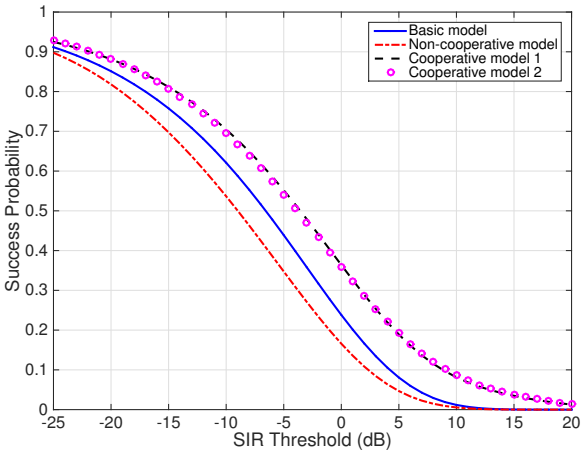

Fig. 10. The SIR distributions of the basic model, the non-cooperative model, the cooperative model 1 and the cooperative model 2 ($\lambda_{\rm p} = 0.1, p = 0.5, b = 1.5, \alpha = 4, u = 1$).

assumptions, the two cooperative techniques have the same performance gain over the non-cooperative model w.r.t. the success probability.

Fig. 10 compares the SIR distribution curves of the four models. As expected, we observe that the performance of the non-cooperative model is the worst while those of the cooperative models are the best, with a horizontal gap of $5-6$ dB. The performance of the two cooperative models is nearly identical. The benefit of cooperation is significant, since by cooperation, some nearby interferers turn into cooperators. Comparing the non-cooperative model and the basic model, we conclude that a horizontal gap of $2-3$ dB can be obtained by silencing some nearby interferers. And by the comparison of the cooperative models and basic model, a horizontal gap of about 3 dB can be gained by adding some nearby cooperators.

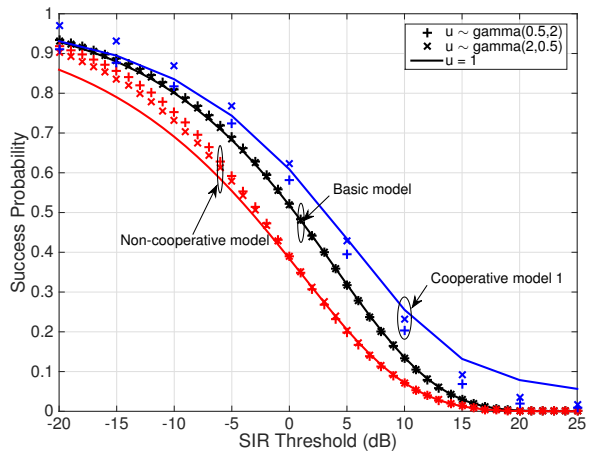

Fig. 11. The SIR distributions of the basic model, the non-cooperative model, and the cooperative model 1, when $u \sim \text{gamma}(0.5, 2)$, $u \sim \text{gamma}(2, 0.5)$ and $u = 1$. ($\lambda_\text{p} = 0.1, p = 0.5, b = 1, \alpha = 4$). The results of the cooperative model 2 are omitted, since they are very similar to those of the cooperative model 1.

B. Random u (Generalized GPP)

We investigate the generalized GPP with u gamma distributed. In Fig. 11, we consider the cases of $u \sim \text{gamma}(0.5, 2)$ and $u \sim \text{gamma}(2, 0.5)$, where $\mathbb{E}[u] = 1$, and show the SIR distributions of the basic model, the non-cooperative model, and the cooperative model 1. For comparison, the case of $u = 1$ is also drawn. The results of the cooperative model 2 are close to those of the cooperative model 1, so they are omitted.

For the basic model, the SIR distribution is invariant under different settings of u, since all points of the GPP are interferers and the interference changes little when the intensity of the GPP remains unchanged with different distribution of u.

For the non-cooperative model, the success probability is improved for random u compared with the deterministic u in the high-reliability regime. The case of $u \sim \text{gamma}(0.5, 2)$ performs better than the case of $u \sim \text{gamma}(2, 0.5)$, which means that as the variance of u becomes larger, the success probability becomes better.

For the cooperative model 1, the success probability for random u is worse than that for the deterministic u in the low-reliability regime, and when the variance of u becomes larger, the benefit from the cooperation is weakened.

VI. Conclusion

In this paper, we first investigated the GPP and used it as a model for point set fitting. The fitted GPP has approximately the same intensity and two-point correlation function as the given point set. Although the GPP cannot model all clustered point processes/sets, it can well model a wide class of them.

We then proposed the application of the GPP in several different wireless network models with and without cooperation and derived the SIR distributions and their bounds for the considered models. The results indicate that the bounds, especially the upper bounds, provide useful approximations that well fit the actual SIR distribution for different operating regimes.

We also showed that by cooperation, the SIR distribution is improved significantly—it has a horizontal gain of more than 5 dB compared with the non-cooperative schemes. Since the two cooperative schemes have similar performance in terms of the SIR distribution, the cooperative scheme without the cyclic delay diversity (scheme 2) is preferred, due to the lower system complexity.

Appendix A
Proof of Corollary 1

Proof: For convenience, let

$$B_1 \triangleq \exp\left(\lambda_\text{p}(1-p)\int_{\mathbb{R}^2}\big(v(x)\ -1\big)\mathrm{d}x\right) \tag{48}$$

and

$$B_2 \triangleq \exp\left(\lambda_\text{p} p\int_{\mathbb{R}^2}\Big(v(x)\int_0^{2\pi} v(x+w(\psi))\frac{1}{2\pi}\mathrm{d}\psi - 1\Big)\mathrm{d}x\right). \tag{49}$$

It follows from Theorem 1 that

$$P_\text{s}(\theta, b, \lambda_\text{p}, \alpha, p) = B_1 B_2. \tag{50}$$

We have

$$\begin{aligned} B_1 &= \exp\left(\lambda_\text{p}(1-p)2\pi\int_0^\infty\Big(\frac{1}{1+sr^{-4}} - 1\Big)r\mathrm{d}r\right) \\ &= \exp\left(-\frac{\pi^2}{2}\lambda_\text{p}(1-p)\sqrt{s}\right) \end{aligned} \tag{51}$$

and

$$B_2 = \exp\Big(\lambda_\text{p} p W\Big), \tag{52}$$

where $W = 2\pi\int_0^\infty\Big(\frac{1}{1+sr^{-4}}\int_0^{2\pi}\frac{1}{1+s(r^2+1+2r\cos\psi)^{-2}}\frac{1}{2\pi}\mathrm{d}\psi - 1\Big)\mathrm{d}r$.

On the one hand,

$$\begin{aligned} W &< \int_0^\infty 2\pi\bigg(\frac{1}{1+sr^{-4}}\Big(\frac{1}{2}\frac{1}{1+s(r^2+1+2r)^{-2}} \\ &\quad + \frac{1}{2}\frac{1}{1+s(r^2+1)^{-2}}\Big) - 1\bigg)r\mathrm{d}r \\ &< \int_0^\infty 2\pi\bigg(\frac{1}{1+sr^{-4}}\Big(\frac{1}{2}\frac{1}{1+s(2(r^2+1))^{-2}} \\ &\quad + \frac{1}{2}\frac{1}{1+s(r^2+1)^{-2}}\Big) - 1\bigg)r\mathrm{d}r \\ &= W_\text{u}(s). \end{aligned} \tag{53}$$

On the other hand,

$$\begin{aligned} W &> \int_0^\infty 2\pi\bigg(\frac{1}{1+sr^{-4}}\Big(\frac{1}{2}\frac{1}{1+s(r^2+1-2r)^{-2}} \\ &\quad + \frac{1}{2}\frac{1}{1+s(r^2+1)^{-2}}\Big) - 1\bigg)r\mathrm{d}r \\ &> \int_0^\infty 2\pi\Big(\frac{1}{1+sr^{-4}}\frac{1}{1+s(r^2+1-2r)^{-2}} - 1\Big)r\mathrm{d}r \\ &= \pi\bigg(-s\int_0^\infty\frac{1}{r^4+s}r\mathrm{d}r - s\int_0^\infty\frac{1}{(r-1)^4+s}r\mathrm{d}r \end{aligned}$$

$$+ s^2 \int_0^\infty \frac{1}{(r^4+s)((r-1)^4+s)} r\mathrm{d}r \Bigg) + \int_0^\infty \pi\big(\frac{1}{1+sr^{-4}} \frac{1}{1+s(r^2+1)^{-2}} - 1\big) r\mathrm{d}r > \pi\Bigg(- s\int_0^\infty \frac{1}{r^4+s} r\mathrm{d}r - s\int_0^\infty \frac{1}{(r-1)^4+s} r\mathrm{d}r + s^2 \int_0^\infty \frac{1}{(r^4+s)((r^2+1)^2+s)} r\mathrm{d}r \Bigg) + \int_0^\infty \pi\big(\frac{1}{1+sr^{-4}} \frac{1}{1+s(r^2+1)^{-2}} - 1\big) r\mathrm{d}r = W_1(s). \quad (54)$$

Combining (50), (51), (52), (53), and (54), we obtain (29) and (29). ∎

Appendix B
Proof of Corollary 3

Proof: Let

$$B_3 = \frac{1-p}{1+p} + \frac{p}{\pi(1+p)} \int_0^{2\pi} \frac{1}{1+s(b^2+1+2b\cos\psi)^{-2}} \mathrm{d}\psi.$$

On the one hand,

$$B_3 < \frac{1-p}{1+p} + \frac{p}{1+p}\Big(\frac{1}{1+s(b^2+1+2b)^{-2}} + \frac{1}{1+s(b^2+1)^{-2}}\Big). \quad (55)$$

On the other hand,

$$B_3 > \frac{1-p}{1+p} + \frac{p}{1+p}\Big(\frac{1}{1+s(b^2+1-2b)^{-2}} + \frac{1}{1+s(b^2+1)^{-2}}\Big). \quad (56)$$

Applying Corollary 1, we obtain the results. ∎

Appendix C
Proof of Corollary 5

Proof: As $h_1 b^{-\alpha} + h_2 c^{-\alpha} \le h_1 b^{-\alpha} + h_2 |b-1|^{-\alpha}$,

$$Q < \mathbb{P}\Big(\frac{h_1 b^{-\alpha} + h_2|b-1|^{-\alpha}}{I} > \theta\Big) = \frac{b^\alpha}{b^\alpha - |b-1|^\alpha} \mathcal{L}_I(\theta|b-1|^\alpha) - \frac{|b-1|^\alpha}{b^\alpha - |b-1|^\alpha} \mathcal{L}_I(\theta b^\alpha) = H(|b-1|), \quad (57)$$

where $H(\cdot)$ is defined in (39). Similarly, as $h_1 b^{-\alpha} + h_2 c^{-\alpha} \ge h_1 b^{-\alpha} + h_2 (b+1)^{-\alpha}$, $Q > H(b+1)$.

Substituting the bounds of Q into (40), we obtain (41) and (42). ∎

Appendix D
Proof of Corollary 6

Proof: The proof for the cooperative model 1 as $u \to 0$ is different from that in Theorem 3 since when the typical receiver is served by two co-located transmitters cooperatively, the desired signal power is not a hypoexponential distribution but an Erlang distribution. We turn to use the following equation to derive the SIR distribution [24].

$$P_{\mathrm{s}}(\theta) = \int_{-\infty}^{\infty} \mathcal{L}_{I_0}(2j\pi\omega) \frac{\mathcal{L}_{P_{\mathrm{sum}}}(-2j\pi\omega/\theta) - 1}{2j\pi\omega} \mathrm{d}\omega, \quad (58)$$

where $\mathcal{L}_{I_0}(s)$ and $\mathcal{L}_{P_{\mathrm{sum}}}(s)$ are the Laplace transform of the interference and the desired signal power respectively. The Laplace transform of the interference $\mathcal{L}_{I_0}(s)$ is given by (32). The Laplace transform of the desired power is given by

$$\begin{aligned}\mathcal{L}_{P_{\mathrm{sum}}}(s) &= \mathbb{E}_{P_{\mathrm{sum}}}(\exp(-sP_{\mathrm{sum}})) \\ &= \frac{1-p}{1+p}\mathbb{E}_h(\exp(-shb^{-\alpha})) \\ &\quad + \frac{2p}{1+p}\mathbb{E}_{h_1,h_2}(\exp(-sh_1 b^{-\alpha} - sh_2 b^{-\alpha})) \\ &= \frac{1-p}{(1+p)(1+sb^{-\alpha})} + \frac{2p}{(1+p)(1+sb^{-\alpha})^2} \\ &= \frac{(1+p)+(1-p)sb^{-\alpha}}{(1+p)(1+sb^{-\alpha})^2}. \end{aligned} \quad (59)$$

Plugging $\mathcal{L}_{I_0}(s)$ and $\mathcal{L}_{P_{\mathrm{sum}}}(s)$ into (58), we get the SIR distribution in Corollary 6. ∎

Appendix E
Proof of Corollary 7

Proof: For the cooperative model 2, as $u \to 0$, by (45), we have

$$P_{\mathrm{s}}(\theta, b, \lambda_{\mathrm{p}}, \alpha, p) \to \frac{1-p}{1+p}\tilde{\mathcal{L}}_{I_o}(\theta b^\alpha) + \frac{2p}{1+p}\tilde{\mathcal{L}}_{I_o}\left(\frac{\theta b^\alpha}{2}\right). \quad (60)$$

Since according to (44), as $u \to 0$,

$$\begin{aligned}\tilde{\mathcal{L}}_{I_o}(s) &\to \exp\left(\lambda_{\mathrm{p}} \int_{\mathbb{R}^2} \Big[\frac{1-p}{1+s\|x\|^{-\alpha}} + \frac{p}{1+2s\|x\|^{-\alpha}} - 1\Big] \mathrm{d}x\right) \\ &= \exp\left(\lambda_{\mathrm{p}}(1-p)\int_{\mathbb{R}^2}\left(\frac{1}{1+s\|x\|^{-\alpha}} - 1\right)\mathrm{d}x \right. \\ &\quad \left. + \lambda_{\mathrm{p}} p \int_{\mathbb{R}^2}\left(\frac{1}{1+2s\|x\|^{-\alpha}} - 1\right)\mathrm{d}x\right) \\ &= \exp\left(-\frac{\pi\lambda_{\mathrm{p}}}{\mathrm{sinc}\,\delta}\left((1-p)s^\delta + p(2s)^\delta\right)\right), \end{aligned} \quad (61)$$

substituting (61) into (60), we obtain (47). ∎

References

[1] A. Guo, Y. Zhong, M. Haenggi, and W. Zhang, "Success probabilities in Gauss-Poisson networks with and without cooperation," in *2014 IEEE International Symposium on Information Theory (ISIT)*, Jun. 2014, pp. 1752–1756.

[2] M. Haenggi, *Stochastic Geometry for Wireless Networks*. Cambridge University Press, 2012.

[3] M. Haenggi, J. G. Andrews, F. Baccelli, O. Dousse, and M. Franceschetti, "Stochastic geometry and random graphs for the analysis and design of wireless networks," *IEEE Journal on Selected Areas in Communications*, vol. 27, no. 7, pp. 1029–1046, Sep. 2009.

[4] H. Nguyen, F. Baccelli, and D. Kofman, "A stochastic geometry analysis of dense IEEE 802.11 networks," in *IEEE INFOCOM 2007*, May 2007, pp. 1199–1207.

[5] Y. Zhong, W. Zhang, and M. Haenggi, "Stochastic analysis of the mean interference for the RTS/CTS mechanism," in *2014 IEEE International Conference on Communications (ICC)*, Jun. 2014, pp. 1996–2001.

[6] R. K. Ganti and M. Haenggi, "Interference and outage in clustered wireless ad hoc networks," *IEEE Transactions on Information Theory*, vol. 55, no. 9, pp. 4067–4086, Sep. 2009.

[7] Y. Zhong and W. Zhang, "Multi-channel hybrid access femtocells: A stochastic geometric analysis," *IEEE Transactions on Communications*, vol. 61, no. 7, pp. 3016–3026, Jul. 2013.

[8] Z. Tong and M. Haenggi, "Throughput analysis for full-duplex wireless networks with imperfect self-interference cancellation," *IEEE Transactions on Communications*, 2015. Accepted. [Online]. Available: http://arxiv.org/pdf/1502.07404v1.pdf

[9] M. Kerscher, "Constructing, characterizing, and simulating Gaussian and higher-order point distributions," *Physical Review E*, vol. 64, no. 5, pp. 056 109(1–17), Oct. 2001.

[10] N. Deng, W. Zhou, and M. Haenggi, "The Ginibre point process as a model for wireless networks with repulsion," *IEEE Transactions on Wireless Communications*, vol. 14, no. 1, pp. 107–121, Jan. 2015.

[11] A. Guo and M. Haenggi, "Spatial stochastic models and metrics for the structure of base stations in cellular networks," *IEEE Transactions on Wireless Communications*, vol. 12, no. 11, pp. 5800–5812, Nov. 2013.

[12] R. K. Milne and M. Westcott, "Further results for Gauss-Poisson processes," *Advances in Applied Probability*, vol. 4, no. 1, pp. 151–176, Apr. 1972.

[13] J. Riihijarvi and P. Mahonen, "Exploiting spatial statistics of primary and secondary users towards improved cognitive radio networks," in *3rd International Conference on Cognitive Radio Oriented Wireless Networks and Communications 2008*, May 2008, pp. 1–7.

[14] D. Lee, H. Seo, B. Clerckx, E. Hardouin, D. Mazzarese, S. Nagata, and K. Sayana, "Coordinated multipoint transmission and reception in LTE-Advanced: deployment scenarios and operational challenges," *IEEE Communications Magazine*, vol. 50, no. 2, pp. 148–155, Feb. 2012.

[15] R. Irmer, H. Droste, P. Marsch, M. Grieger, G. Fettweis, S. Brueck, H.-P. Mayer, L. Thiele, and V. Jungnickel, "Coordinated multipoint: Concepts, performance, and field trial results," *IEEE Communications Magazine*, vol. 49, no. 2, pp. 102–111, Feb. 2011.

[16] K. Huang and J. G. Andrews, "A stochastic-geometry approach to coverage in cellular networks with multi-cell cooperation," in *2011 IEEE Global Communications Conference (GLOBECOM)*, Dec. 2011, pp. 1–5.

[17] J. Liu, W. Chen, Z. Cao, and Y. J. Zhang, "Delay optimal scheduling for cognitive radios with cooperative beamforming: A structured matrix-geometric method," *IEEE Transactions on Mobile Computing*, vol. 11, no. 8, pp. 1412–1423, Aug. 2012.

[18] F. Baccelli and A. Giovanidis, "A stochastic geometry framework for analyzing pairwise-cooperative cellular networks," *IEEE Transactions on Wireless Communications*, vol. 14, no. 2, pp. 794–808, Feb. 2015.

[19] R. Tanbourgi, S. Singh, J. Andrews, and F. Jondral, "A tractable model for noncoherent joint-transmission base station cooperation," *IEEE Transactions on Wireless Communications*, vol. 13, no. 9, pp. 4959–4973, Sep. 2014.

[20] G. Nigam, P. Minero, and M. Haenggi, "Coordinated multipoint joint transmission in heterogeneous networks," *IEEE Transactions on Communications*, vol. 62, no. 11, pp. 4134–4146, Nov. 2014.

[21] D. S. Newman, "A new family of point processes which are characterized by their second moment properties," *Journal of Applied Probability*, vol. 7, no. 2, pp. 338–358, Aug. 1970.

[22] C.-H. Lee and M. Haenggi, "Interference and outage in Poisson cognitive networks," *IEEE Transactions on Wireless Communications*, vol. 11, no. 4, pp. 1392–1401, Apr. 2012.

[23] M. Afshang, H. S. Dhillon, and P. H. J. Chong, "Coverage and area spectral efficiency of clustered device-to-device networks," in *2015 IEEE Global Communications Conference (GLOBECOM)*, 2015. Submitted.

[24] F. Baccelli, B. Blaszczyszyn, and P. Muhlethaler, "Stochastic analysis of spatial and opportunistic Aloha," *IEEE Journal on Selected Areas in Communications*, vol. 27, no. 7, pp. 1105–1119, Sep. 2009.